Hindawi
Journal of Chemistry
Volume 2023, Article ID 7148988, 12 pages
https://doi.org/10.1155/2023/7148988

Research Article

Functionalized Magnetite Nanoparticles Using Two New Ionic Liquids for Efficient Oil Spill Cleanup

Noorah A. Faqihi, Mahmood M. S. Abdullah, Mohd Sajid Ali, Hamad A. Al-Lohedan, and Zainab M. Almarhoon

Department of Chemistry, College of Science, King Saud University, P.O. Box 2455, Riyadh 11451, Saudi Arabia

Correspondence should be addressed to Mahmood M. S. Abdullah; maltaiar@ksu.edu.sa

Received 15 November 2022; Revised 24 January 2023; Accepted 23 February 2023; Published 2 March 2023

Academic Editor: Zhaoqiang Zhang

Recently, magnetite nanoparticles (MNPs) have gained great attention for oil spill cleanup due to their unique properties, e.g., high oil removal efficiency, high surface area, and response to an external magnetic field. The efficiency of MNPs for oil spill uptake can be enhanced by functionalizing their surface using different materials. Furthermore, the functionalization of MNP surface using these materials promotes their chemical stability. This study aims to functionalize the surface of magnetite nanoparticles (MNPs) using two newly synthesized hydrophobic ionic liquids (ILs) and apply them for oil spill cleanup. ILs were synthesized by the reaction of glycidyl-4-nonyl ether (GE) with fatty amines, either octadecylamine (OA) or dodecylamine (DA), to yield the corresponding amines, GEOA and GEDA, respectively. GEOA and GEDA were quaternized with acetic acid (AA) to produce the corresponding ILs, GEOA-IL and GEDA-IL. The produced ILs, GEOA-IL and GEDA-IL, were applied for the surface modification of magnetite nanoparticles (MNPs), producing surface-modified MNPs, GO-MNPs and GD-MNPs, respectively. GO-MNPs and GD-MNPs were characterized using Fourier transform infrared, X-ray diffraction, transmission electron microscopy, dynamic light scattering, contact angle, and vibrating sample magnetometer. Their oil removal efficiency (ORE) was investigated at different MNP : crude oil ratios ranging from 1 : 1–1 : 50. GO-MNPs and GD-MNPs showed high ORE even at low MNP ratios. Furthermore, GO-MNPs showed higher oil removal efficiency than GD-MNPs, which may be explained using GEOA-IL containing a longer alkyl chain for MNP surface modification in comparison to GEDA-IL. Furthermore, GO-MNPs and GD-MNPs displayed excellent reusability in five cycles, with a slight decrease in ORE with increasing cycles.

1. Introduction

Oil spills in aquatic environments impose a major threat on these environments, where a significant portion of oil is emulsified, making its separation from the water phase extremely difficult. Oil spills affect the seaside flora, fauna such as birds and bivalve mollusks, and human health due to oil-contaminated food via the food chain. Some oil components in contaminated food can be considered a carcinogen [1, 2]. In addition, the contact area between water and the atmosphere is reduced as a result of oil spills affecting the chemical oxygen demand (COD) and biochemical oxygen demand (BOD), thereby hindering the respiration of aerobic marine organisms and photosynthesis in marine plants [3]. Oil spills occur during oil extraction, transportation, and oil transfer between vessels, resulting in tremendous environmental impacts [3, 4]. From 2000 to 2011, over 224.000 tons of oil were released into the seas and oceans [5]. Although a range of oil removal methods is available, including physical, chemical, and biochemical, these methods have some limitations, such as high cost, low efficiency, and the fact that they contribute to other secondary pollutants [6]. There is an urgent need for a technique that has the potential to overcome all of these limitations of conventional techniques without increasing energy consumption. This technique does not contribute to pollution, is easy to use regardless of the weather conditions, and is efficient [7].

Recently, nanotechnology was applied significantly to combat the oil spill disaster. Several types of nanomaterials were reported for oil spill cleanup, including organic nanoclays, iron oxide (Fe_3O_4 and Fe_2O_3) nanoparticles, carbon-based nanoparticles (graphite, graphene, carbon nanotubes, etc.), and TiO_2 [7]. In particular, magnetite nanoparticles (MNPs) are characterized by high oil removal efficiency. Using MNPs, oil can be easily recovered from the water's surface. Furthermore, MNPs are characterized by their biodegradability, nonsinking properties, and reusability [8–10]. Surface modification of MNPs improves their stability by creating a protective film on their surface that prevents air oxidation. In addition, it prevents their agglomeration due to their magnetic nature and enhances their efficiency in removing oil spills [6, 11]. Several organic and inorganic materials have been used to modify the surface of MNPs [12]. The use of hydrophobic materials, particularly for the surface modification of MNPs, often enhances their dispersity in oil more than in water. This increases their interaction with oil components and thereby increases their oil removal efficiency [13].

Ionic liquids are organic salts having melting points lower than 100°C. ILs have a variety of unique properties, e.g., low melting point and high mechanical and thermal stability, which make them suitable for MNP surface modification. Furthermore, due to their ionic nature, these materials can work efficiently even in harsh saline conditions where conventional materials cannot work. Limited studies reported the application of surface-modified MNPs using ionic liquids (ILs) for oil spill cleanup. The surface-modified MNPs using ILs exhibited excellent performance in oil spill cleanup compared to MNPs modified using other organic materials [14, 15].

Herein, two newly synthesized hydrophobic ILs were synthesized and used to modify MNP surfaces. First, glycidyl-4-nonyl ether (GE) was reacted with either octadecylamine (OA) or dodecylamine (DA) through a ring-opening reaction to obtain the corresponding amines, GEOA and GEDA. Next, the produced amine, GEOA or GEDA, was quaternized with acetic acid (AA) to yield the corresponding ILs, GEOA-IL and GEDA-IL. Finally, the as-synthesized ILs, GEOA-IL and GEDA-IL, were used to functionalize the surface of MNPs to obtain GO-MNPs and GD-MNPs, respectively. The chemical structures, thermal stability, particle size, morphology, and magnetic properties of the as-synthesizedGO-MNPs and GD-MNPs were investigated using two different methods. In addition, the efficiency of GO-MNPs and GD-MNPs for oil removal was evaluated using different MNP : crude oil ratios.

2. Experimental

2.1. Materials. Dodecylamine (DA), octadecylamine (OA), glycidyl-4-nonyl ether (GE), iron (III) chloride, anhydrous ($FeCl_3$), iron (II) chloride tetrahydrate ($FeCl_2.4H_2O$), ammonium hydroxide (NH_4OH), acetic acid (AA), sodium chloride, isopropyl alcohol, and ethanol were supplied by Sigma-Aldrich and used without further purification.

Crude oil was supplied by Aramco, Riyadh, Saudi Arabia. Its API and contents (weight%) of saturates, aromatics, resins, and asphaltenes (SARA) are 20.8°, 16.3, 25.3, 48.1, and 8.3, respectively. Its full specification was reported in our earlier work [16]. Brine solution (35 g/L) was prepared in our lab using double distilled water and sodium chloride.

2.2. Synthesis of GEOA-IL and GEDA-IL. Glycidyl-4-nonyl ether (GE) (3 g, 10.85 mM) was stirred and heated with either OA (2.62 g, 10.85 mM) or DA (2.01 g, 10.85 mM) at 100°C in a nitrogen atmosphere for 3 h to obtain the corresponding amines, GEDA and GEOA [17]. Next, GEDA or GEOA was stirred and heated with equimolar AA at 100°C for 5 h in a nitrogen atmosphere. The obtained mixtures were cooled to room temperature and dissolved separately in isopropyl alcohol, and the unreacted AA was salted out using a supersaturated sodium chloride solution. Finally, the organic layer was separated, and isopropyl alcohol was evaporated under reduced pressure to obtain the corresponding ILs, GEOA-IL and GEDA-IL, as viscous liquids with yields of 98.8% and 98.4%, respectively. The GEOA-IL and GEDA-IL synthesis route is presented in Scheme 1.

2.3. Synthesis of GO-MNPs and GD-MNPs. For the synthesis of GO-MNPs and GD-MNPs, IL solution (4 g of either GEOA-IL or GEDA-IL dissolved in 200 mL of ethanol) was mixed and stirred with $FeCl_3$ and $FeCl_2$ solution (6.36 g of $FeCl_3$ and 3.9 g of $FeCl_2$ dissolved in 200 mL of distilled water) in a three-neck bottom flask supplied with a nitrogen inlet and thermometer. The obtained mixture was heated at 50°C, and ammonium hydroxide solution (28%) was added dropwise while stirring continuously, reaching pH 10. After adding NH_4OH, the mixture was stirred for 1 h to ensure the reaction completeness. The surface-modified MNPs were separated using an external magnet, washed several times with ethanol, followed by distilled water, and dried at ambient temperature [18]. The overall reaction of the preparation of the surface-modified MNPs can be carried out according to the following equation:

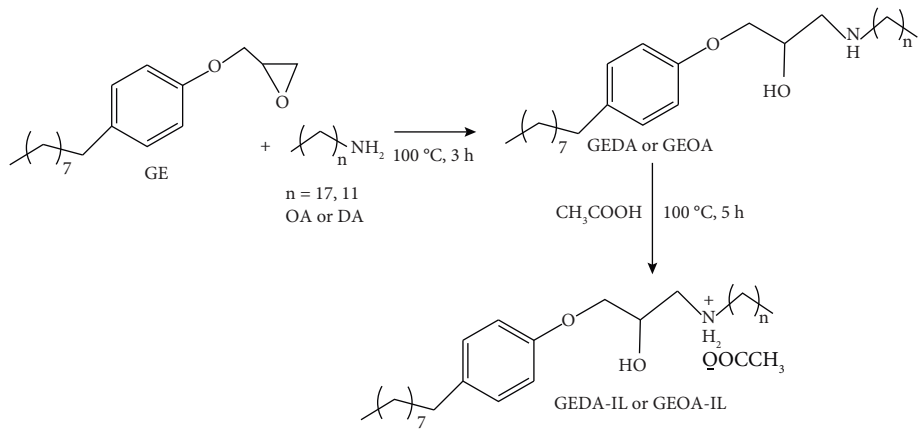

Scheme 1: Synthesis routes of GEOA-IL and GEDA-IL.

$$\text{IL} + \text{Fe}^{2+} + \text{Fe}^{3+} + \text{H}_2\text{O} + \text{NH}_3 \longrightarrow \frac{\text{IL}}{\text{Fe}_3\text{O}_4}. \quad (1)$$

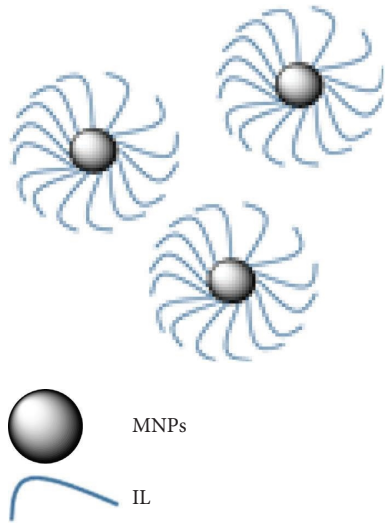

2.4. Characterization. Fourier transform infrared (FTIR) and proton nuclear magnetic resonance (^{1}H-NMR) were performed to confirm the chemical structures of the as-synthesized ILs. In addition, FTIR and X-ray diffraction (XRD) were conducted to confirm the chemical structures of the as-synthesizedGO-MNPs and GD-MNPs. Transmission electron microscopy (TEM) was used to investigate the morphology of GO-MNPs and GD-MNPs. Dynamic light scattering (DLS) was used to investigate the particle size (PS) of GO-MNPs and GD-MNPs in ethanol. A vibrating sample magnetometer (VSM) was employed to confirm the magnetic properties of GO-MNPs and GD-MNPs.

The hydrophobicity of GO-MNPs and GD-MNPs was examined using contact angle (CA) measurements as follows: 0.5 g of either GO-MNPs or GD-MNPs was dispersed in a small amount of chloroform and spread over the glass slide surface, and then chloroform was evaporated. A thin, dry film was obtained on the glass slide surface by repeating this step many times. The CA of seawater droplets on the prepared glass slide was evaluated using a drop-shape analyzer [19].

2.5. Efficiency of GO-MNPs and GD-MNPs for Oil Spill Removal. In a 100 mL beaker, 200 mg of heavy crude oil sample was injected on the surface of 70 mL of seawater. Over the surface of crude oil, different amounts of MNPs samples (ranging from 4 mg to 200 mg) were spread out and kept for 10 minutes. Then, a block neodymium magnet (4300 Gauss) covered with a known weight plastic film was used to remove MNPs with adsorbed oil on their surfaces. Both the MNPs with adsorbed oil on their surfaces and the plastic film were recovered. They were frozen, lyophilized for 24 h to get rid of dragged water, and finally weighed to calculate the mass of removed oil [3]. All experiments were conducted in triplicate. This method was considered method A, and the oil removal efficiency (ORE) was calculated using the following equation:

$$\text{ORE\%} = \frac{\text{mass of collected oil}}{\text{mass of original oil}} \times 100. \quad (2)$$

The ORE was also evaluated by a different method. First, 10 minutes after the dispersion of MNPs on the crude oil surface, the MNPs with adsorbed oil were collected on the inside wall of the beaker, where the external magnet was placed outside the beaker's wall. Therefore, the MNPs with adsorbed oil were collected on the inside wall of the beaker. Then, the water and residual crude oil were poured into a separating funnel keeping external magnet attached to the wall of the beaker, and the residual oil was extracted with chloroform. In the following step, chloroform was evaporated under reduced pressure, and the mass of the residual crude oil was recorded. This method was considered method B, and the ORE was calculated using the following equation:

$$\text{ORE\%} = \frac{\text{mass of original oil} - \text{mass of residu al oil}}{\text{mass of original oil}} \times 100. \quad (3)$$

For reusing GO-MNPs and GD-MNPs, the crude oil was removed from the surface of the collected MNPs by washing them using chloroform, followed by acetone. Finally, the obtained MNPs were dried in the air and reused in a new cycle.

3. Results and Discussion

3.1. Chemical Structures of the As-Synthesized ILs and MNPs. The chemical structures of the as-synthesized ILs, GEOA-IL and GEDA-IL, were confirmed using FTIR and ^{1}H-NMR as presented in Figures 1(a) and 2, respectively. In Figure 1, the stretching absorption bands of hydroxyl groups appear at 3316 cm^{-1}. C-H aliphatic's stretching and bending bonds appear at 2924, 2855 cm^{-1}, and 1465 cm^{-1}. The stretching absorption bands of aromatic bonds, a =C-H and C=C, are assigned at 3050 cm^{-1}, 1608 cm^{-1}, and 1513 cm^{-1}, respectively. The stretching absorption bands of aliphatic and aromatic C-O are observed at 1120 cm^{-1} and 1042 cm^{-1}, respectively. In the ^{1}H-NMR spectra (Figures 2(a) and 2(b)), the protons of the alkylamine and alkyl side chain of GE resonated between 0.7 and 3 ppm [17]. The protons of the acetate group, $+NCH_2$ and OCH, appear at 1.97 ppm, 3.95 ppm, and 4.1 ppm, respectively. Furthermore, the protons of the phenyl ring and $+NH_2$ are observed at 6.8 ppm, 7.2 ppm, and 8.8 ppm, respectively.

The chemical structures of as-synthesized MNPs, GO-MNPs and GD-MNPs, were also investigated using FTIR and XRD. The FTIR spectra of GO-MNPs and GD-MNPs (Figure 1(b)) show the same functional groups as GEOA-IL and GEDA-IL with low intensity, confirming the functionalization of MNP surfaces with these ILs. Furthermore, the appearance of new intensive bands at 568 cm^{-1} and 565 cm^{-1} for GO-MNPs and GD-MNPs, respectively (Fe-O), confirms the formation of pure magnetite without any other iron oxides. Figure 3 represents the XRD pattern of GD-MNPs and GO-MNPs. The figure shows apparent characteristic peaks at 2 theta values of 30.6°, 36.2°, 43.3°, 54.4°, 57.4°, 62.8°, and 75.1° corresponding to the cubic spinel structure of Fe_3O_4 as (220), (311), (400), (422), (511), and (622) [20]. The data indicate that the crystal structures of GO-MNPs and GD-MNPs were not affected by their surface modification with the constituents of as-synthesized ILs.

3.2. Thermal Stability of GO-MNPs and GD-MNPs. The TGA thermogram of GO-MNPs and GD-MNPs is presented in Figure 4. As shown in the figure, there is no weight loss up to 200°C. The data also showed that the degradation of GO-MNPs and GD-MNPs occurs in two main steps. The first primary degradation step was between 200°C and 420°C which can be linked to the degradation of IL organic constituents. The second degradation step was between 550°C and 700°C. The degradation in this region is due to changes in the inorganic core where the MNPs at such temperature are converted to γ-hematite or nonstoichiometric wustite ($Fe_{(1-x)}O$) [21]. The percentage of weight loss for GO-MNPs and GD-MNPs at 800°C was 11% and 13%, respectively, which reflects the relative decrease in the amount of IL on the MNP surface in the case of GO-MNPs as compared to that of GD-MNPs (Figure 4).

3.3. Particle Size of GO-MNPs and GD-MNPs. Figures 5(a) and 5(b) represent the TEM images of GO-MNPs and GD-MNPs. As seen in the figure, the MNPs are arranged in cluster form, which could be attributed to their magnetic nature, where these particles attract each other [22]. The TEM images also showed that the MNPs appeared in irregular shapes with average diameters of 10 nm and 8.5 nm for GO-MNPs and GD-MNPs, respectively. The particle size (PS) of GO-MNPs and GD-MNPs was also measured in ethanol using the DLS technique, as depicted in Figures 6(a) and 6(b). The average diameters determined by DLS for GO-MNPs and GD-MNPs are 690.7 nm and 193.2 nm, respectively. The difference in the particle size values measured by TEM and DLS reflects the behavior of GO-MNPs and GD-MNPs in ethanol, where they tend to agglomerate in clusters due to their magnetic nature. Furthermore, the increase in the PS of GO-MNPs measured by DLS can be attributed to an increased magnetization value that enhances their attraction to each other compared to that of GD-MNPs, as will be explained later.

3.4. Contact Angle Measurement. The hydrophobicity of the MNPs used for oil spill removal is crucial because it supports the dispersion of these nanoparticles in crude oil. It also reduces their water dispersion and thereby enhances their interaction with crude oil constituents. CA measurements are one of the most common methods of determining hydrophobicity. The high CA values of water droplets on surfaces (>90°) indicate the hydrophobicity of these surfaces, and as the hydrophobicity increases, the CA value increases. Herein, the CA of water droplets on the surface of GO-MNPs and GD-MNPs was measured as it was reported in the Experimental section. Figures 7(a) and 7(b) show the CA of seawater droplets on the surfaces of GO-MNPs and GD-MNPs, respectively. As shown in the figure, the CA values of seawater droplets on the surfaces of GO-MNPs and GD-MNPs were 128.4° and 120.3°, respectively. These values indicated an increase in the hydrophobicity of GO-MNPs and GD-MNPs. This increase in hydrophobicity can be related to the functionalization of MNPs with hydrophobic ILs. In addition, GO-MNPs showed higher hydrophobicity than GD-MNPs due to the presence of longer alkyl chains in GEOA-IL used for the functionality of MNPs surfaces compared to those present in GEDA-IL.

3.5. Magnetic Characterization. To retrieve the MNPs with oil adsorbed on their surfaces, they must respond to an external magnetic field. GO-MNPs and GD-MNPs were successfully collected using an external magnetic field during this study. The response of these MNPs to an external magnetic field was also investigated using VSM, as shown in Figure 8. As depicted in the figure, the magnetization values are 56.7 emu/g and 49.4 emu/g for GO-MNPs and GD-MNPs, respectively. These data indicated the ability of

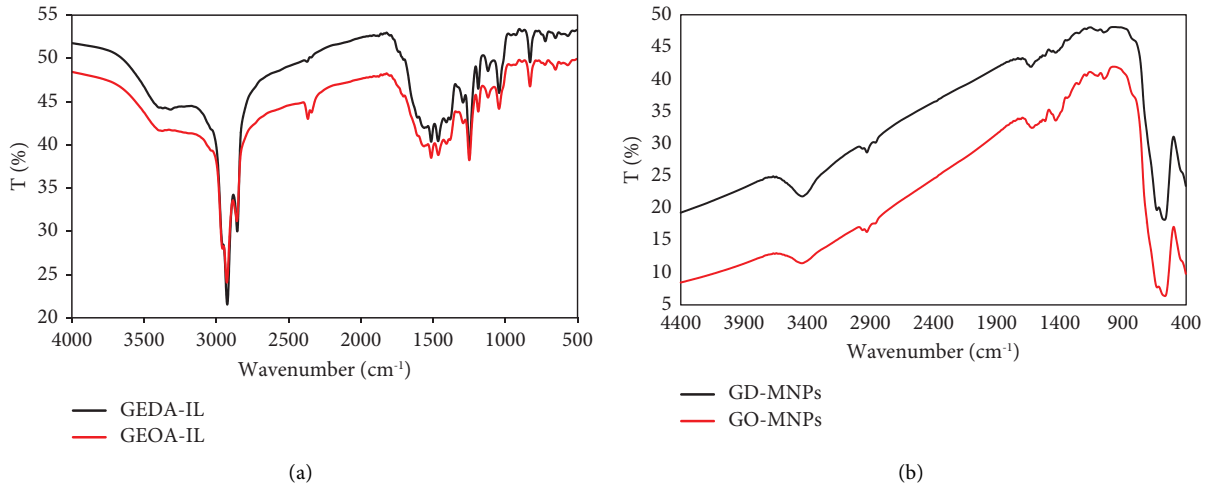

Figure 1: FTIR spectra of (a) ILs, GEDA-IL and GEOA-IL, and (b) MNPs, GD-MNPs and GO-MNPs.

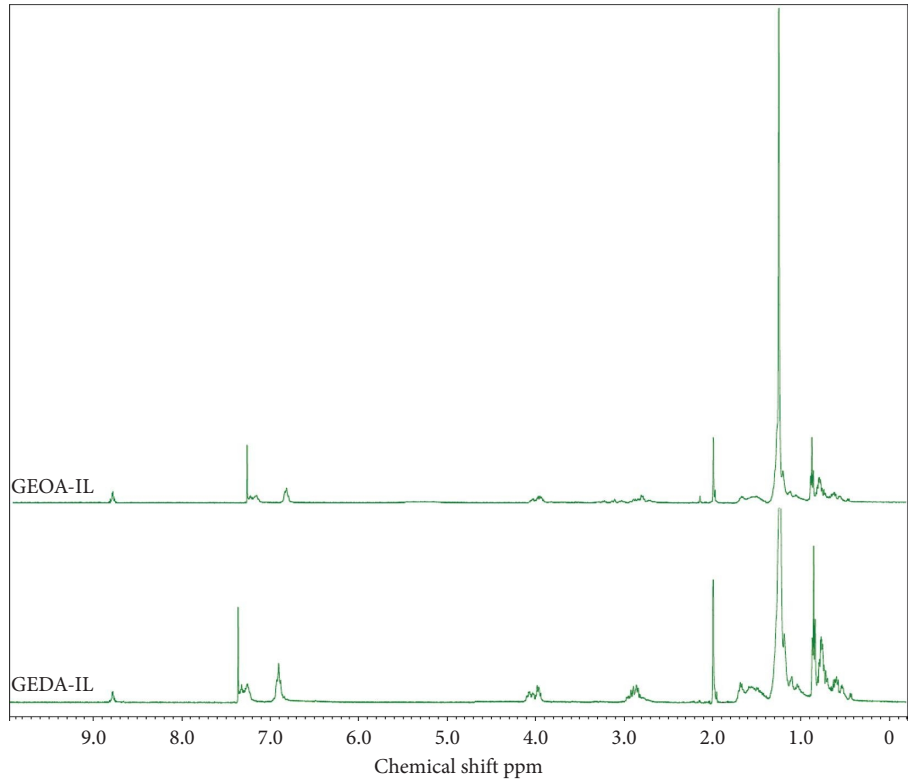

Figure 2: ^{1}H-NMR of GEOA-IL and GEDA-IL.

GO-MNPs and GD-MNPs to respond to the external magnetic field.

3.6. Oil Removal Efficiency (ORE) of GO-MNPs and GD-MNPs. As reported earlier, ILs used for MNP surface modification significantly enhance MNPs' performance for oil spill uptake compared to other organic materials [14, 15]. Therefore, in this work, the newly synthesized ILs, GEOA-IL and GEDA-IL, were employed for the MNPs' surface modification to enhance their performance for oil spill uptake. The obtained surface-modified MNPs, GO-MNPs and GD-MNPs, showed effective dispersion in low polar solvents with no dispersion in water and response to an external magnetic field, indicating their ability to serve in crude oil removal. Herein, the ORE values of GO-MNPs and GD-MNPs were evaluated using two different methods, as reported in the Experimental section. Figures 9(a) and 9(b) show the ORE at different ratios of GO-MNPs and GD-MNPs using methods A and B, respectively. As shown in the

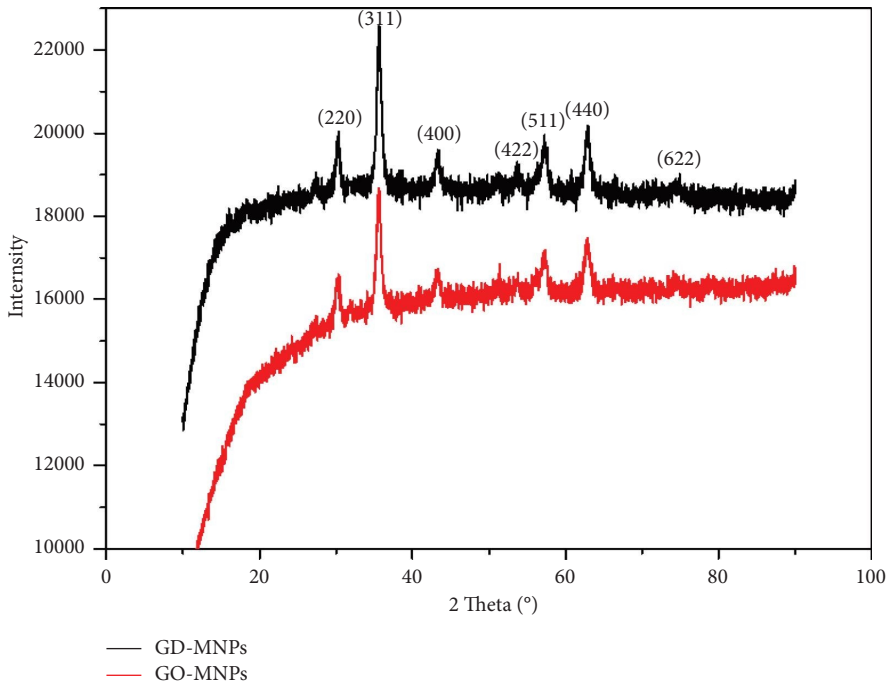

Figure 3: XRD pattern of GD-MNPs and GO-MNPs.

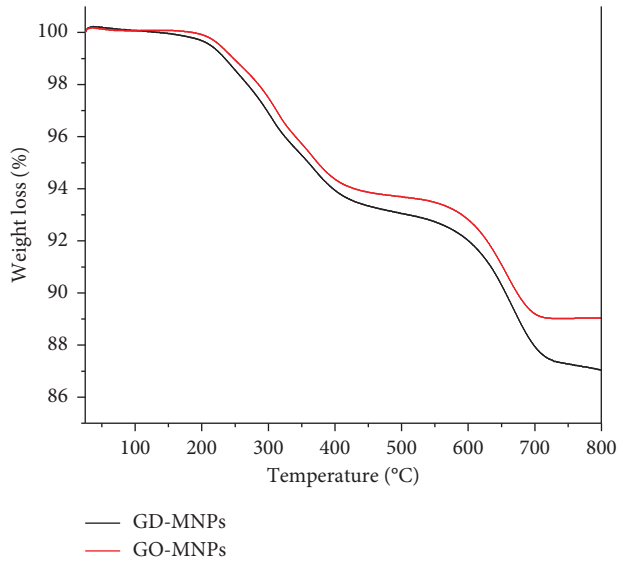

Figure 4: TGA analysis of GO-MNPs and GD-MNPs.

figure, the ORE increased as the ratio of MNPs increased. In addition, GO-MNPs exhibited higher ORE than GD-MNPs at all ratios. This could be linked to an increase in hydrophobicity of GO-MNPs compared to GD-MNPs due to the presence of longer alkyl chains in GEOA-IL used for the functionality of MNP surface compared to those present in GEDA-IL. The data also showed the differences between the ORE values measured using methods A and B. At MNP : crude oil ratios of 1 : 1 and 1 : 2, the ORE values seem to be similar, while with a decrease in the MNP ratios, the difference increased significantly, whereas the ORE values in method B decreased with a decrease in the MNP ratios. In method B, with a decrease in the MNP ratio, the attraction between these nanoparticles and the external magnetic field decreases where the magnet is placed outside the beaker. This leads to an increase in the distance between MNPs and the magnet.

Table 1 compares the MNPs' ORE values in the current work, the ORE values of untreated MNPs, and the ORE values of surface-modified MNPs using different organic materials reported earlier. The data showed that the surface-modified MNPs, GO-MNPs and GD-MNPs, showed higher

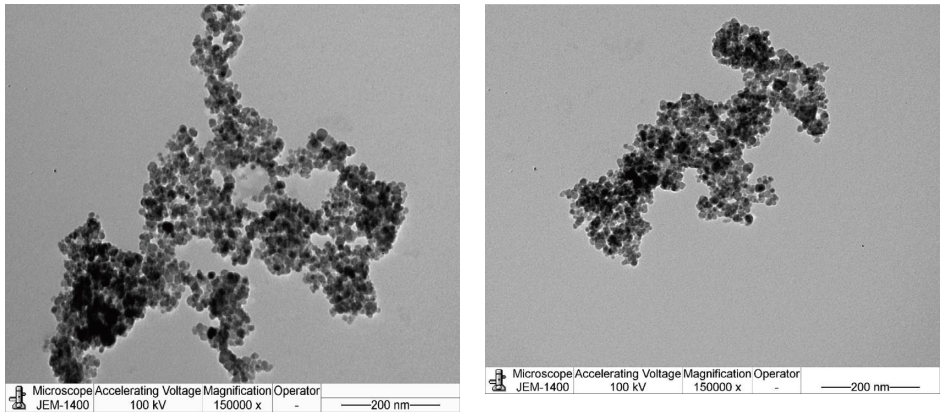

(a) (b)

Figure 5: TEM images of (a) GO-MNPs and (b) GD-MNPs.

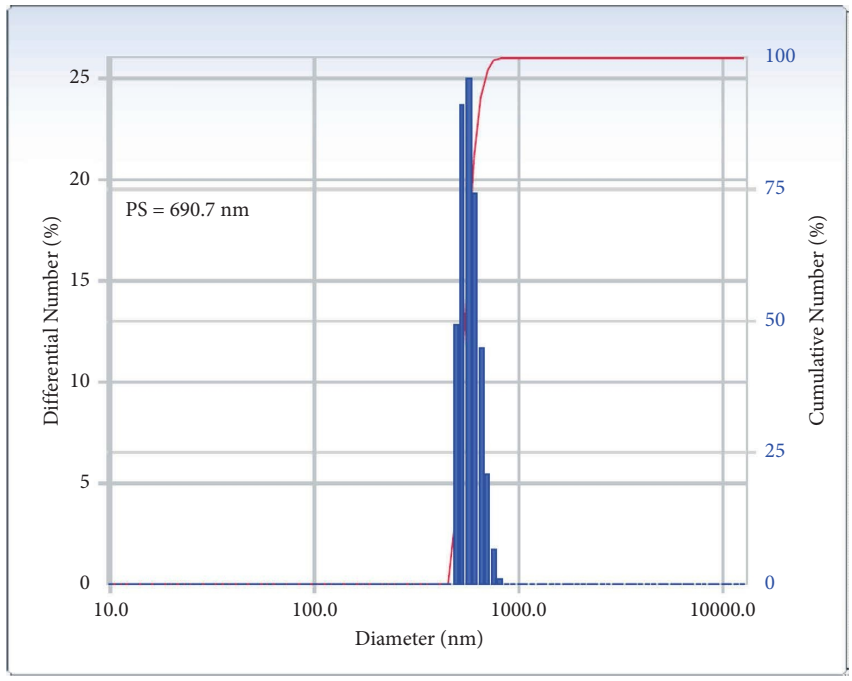

(a)

Figure 6: Continued.

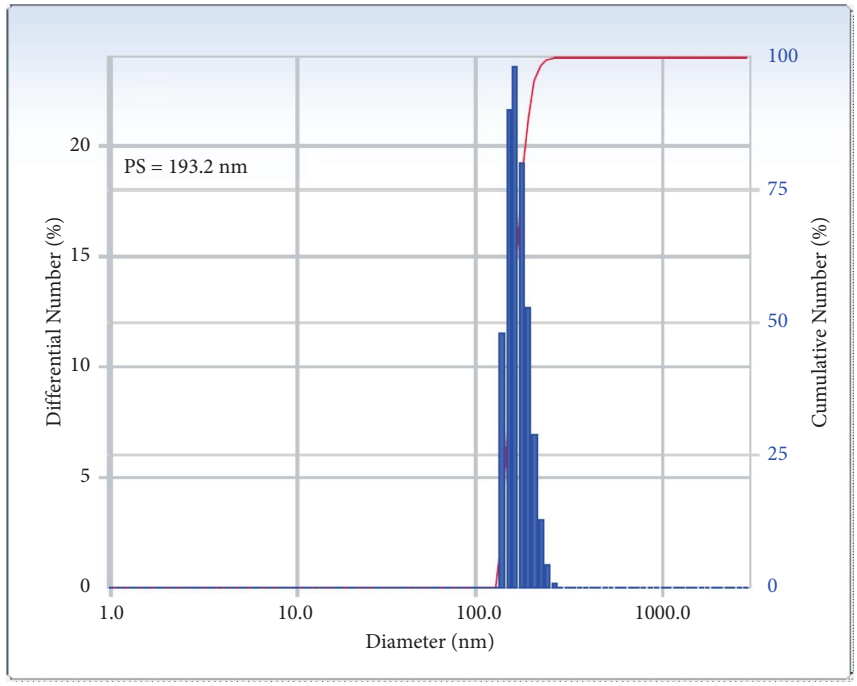

(b)

Figure 6: DLS of (a) GO-MNPs and (b) GD-MNPs.

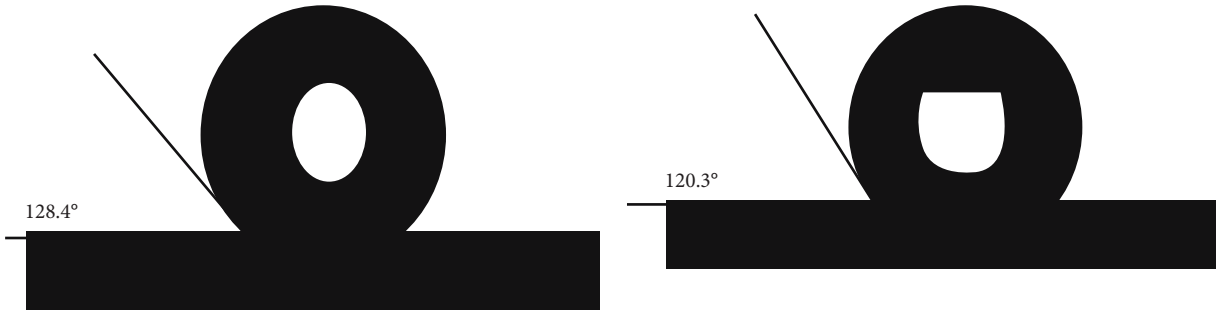

(a) (b)

Figure 7: Contact angles of seawater droplets on (a) GO-MNP and (b) GD-MNP surfaces.

ORE values than the untreated MNPs. These data indicated the role of GEOA-IL and GEDA-IL in enhancing the efficiency of the surface-modified MNPs for oil spill uptake. Furthermore, the surface-modified MNPs using ILs in this work and those reported earlier achieved higher ORE values than the surface-modified MNPs using other organic materials. These data reflect the role of ILs in improving the dispersity of MNPs in crude oil and their interaction with crude oil constituents, thus enhancing their performance for oil spill uptake.

Figures 10(a)–10(d) show the oil spilled over seawater, the dispersed GO-MNPs over the crude oil at MNP : crude oil ratio of 1 : 2, and the cleanness of seawater after the removal of oil with methods A and B, respectively. According to the figure, in both methods, GO-MNPs were highly effective for oil removal and obtaining clean seawater.

3.7. Reusability of GO-MNPs and GD-MNPs. The reusability of MNPs is one of the most significant parameters since they can be easily retrieved with an external magnetic field. Therefore, the reusability of GO-MNPs and GD-MNPs was investigated in five cycles, as presented in Figure 11, using a ratio of 1 : 4 (MNP :crude oil). The data indicated that the ORE of MNPs is reduced slightly with increasing cycles. For example, in the first cycle, the ORE values were 96% and 93%

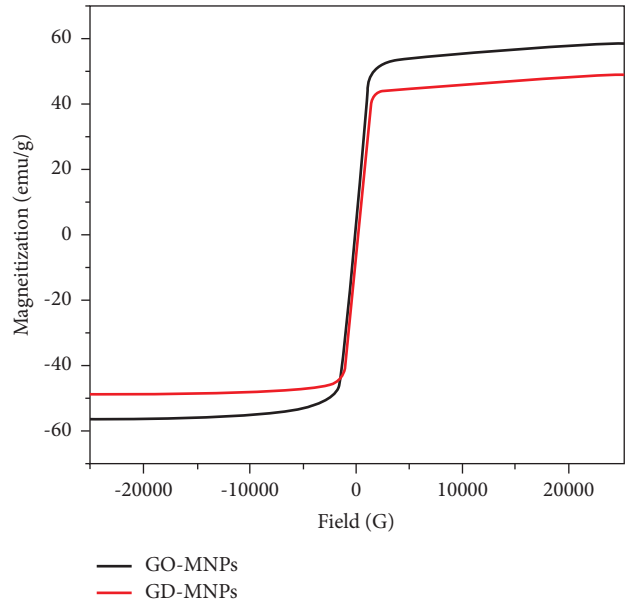

Figure 8: VSM magnetization curve of GO-MNPs and GD-MNPs.

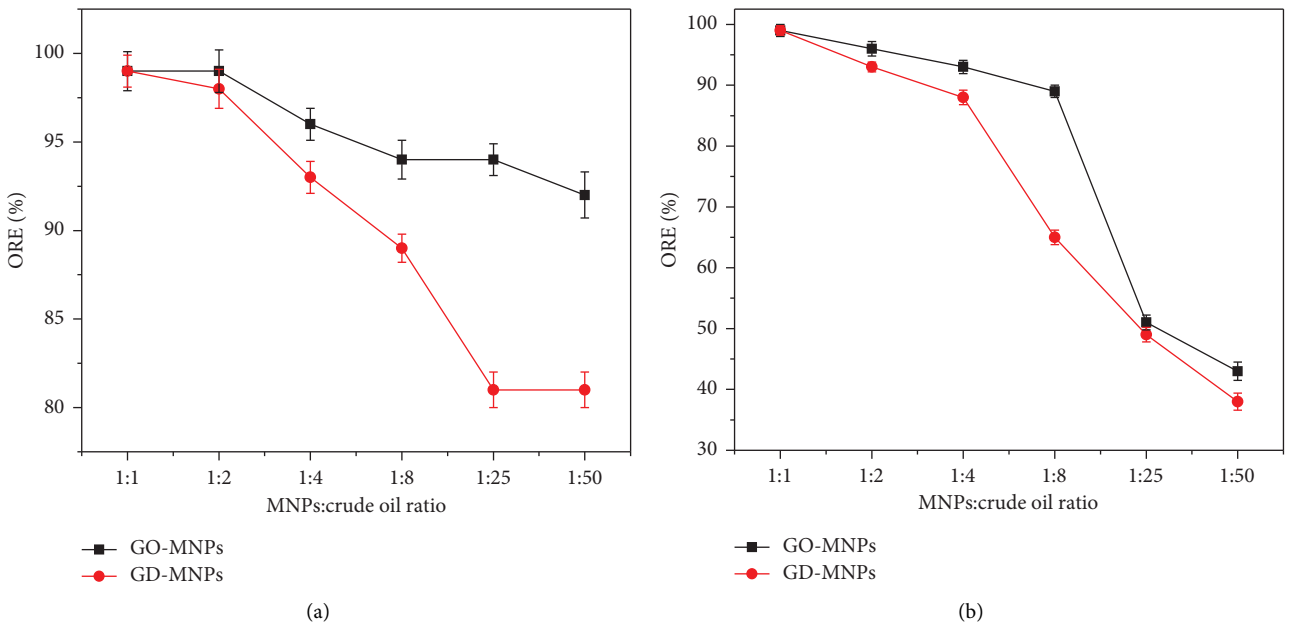

Figure 9: Oil removal efficiency (ORE%) of GO-MNPs and GD-MNPs using (a) method A and (b) method B.

Table 1: Comparison between the ORE values of MNPs prepared in the current work, ORE values of untreated MNPs, and ORE values of surface-modified MNPs using different organic materials.

Symbol/organic material used for surface modification	ORE% MNP : crude oil ratio					Reference
	1 : 1	1 : 8	1 : 10	1 : 25	1 : 50	
Untreated MNPs	45		10			[23]
GO-MNPs/ammonium-based IL	99	94		94	92	Current work
GD-MNPs/ammonium-based IL	98	89		81	81	Current work
DT-MNMs/IL	99	98		95	87	[14]

Table 1: Continued.

Symbol/organic material used for surface modification	ORE% MNP : crude oil ratio					Reference
	1 : 1	1 : 8	1 : 10	1 : 25	1 : 50	
TP-MNMs/IL	99	98		95	90	[14]
AMO/1-allyl-3-methylimidazolium oleate	100			95	90	[14]
SAS-MPKI/modified asphaltene	92		90	88	80	[24]
SAS-MPNS/modified asphaltene	98		94	90	85	[24]
OA-MNPs/amide of alginate	96		93	87	78	[16]
DA-MNPs/amide of alginate	90		87	75	67	[16]
APC-MNPs/plant extract	81		78	74	70	[19]
APH-MNPs/plant extract	92		90	88	83	[19]
Fe_3O_4/RMA-750/modified nonionic rosin surfactant	90		92			[25]

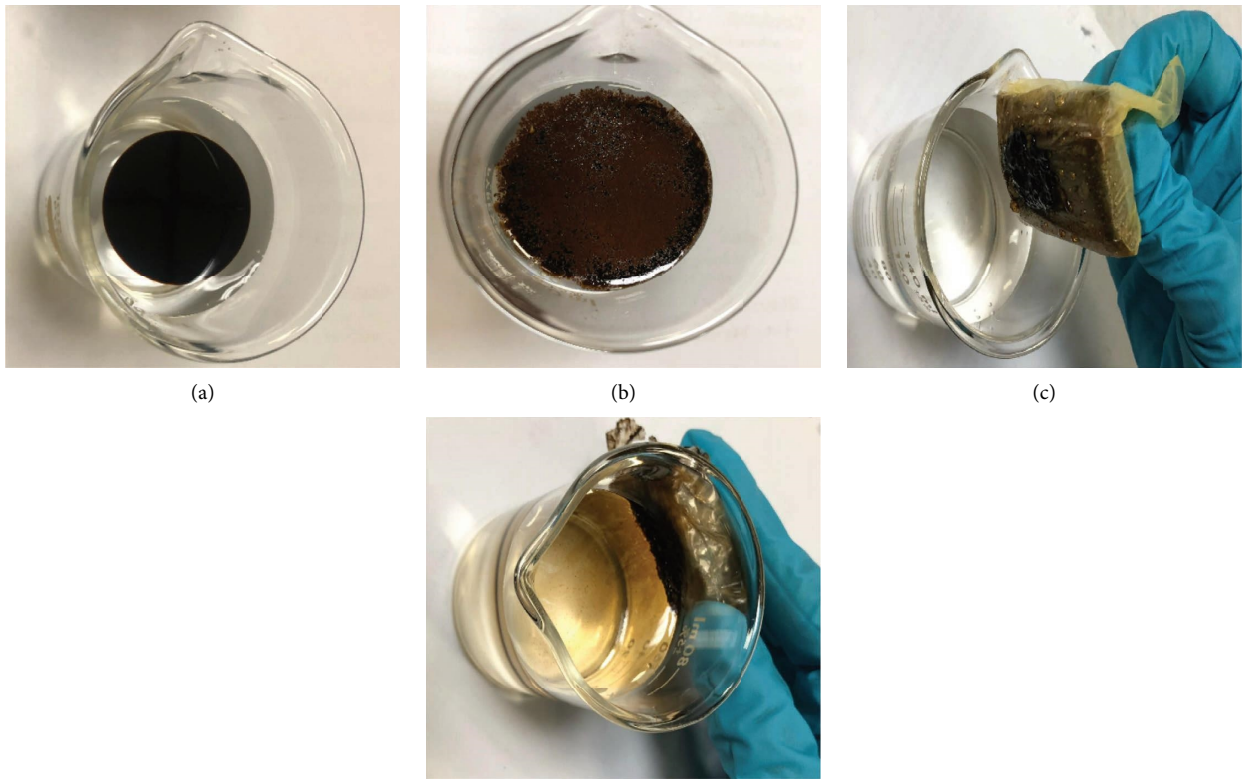

(a) (b) (c) (d)

Figure 10: Optical images of (a) oil spilled over seawater, (b) dispersed GO-MNPs over the crude oil at MNP : crude oil ratio of 1 : 2, (c) oil removal using method A, and (d) oil removal using method B.

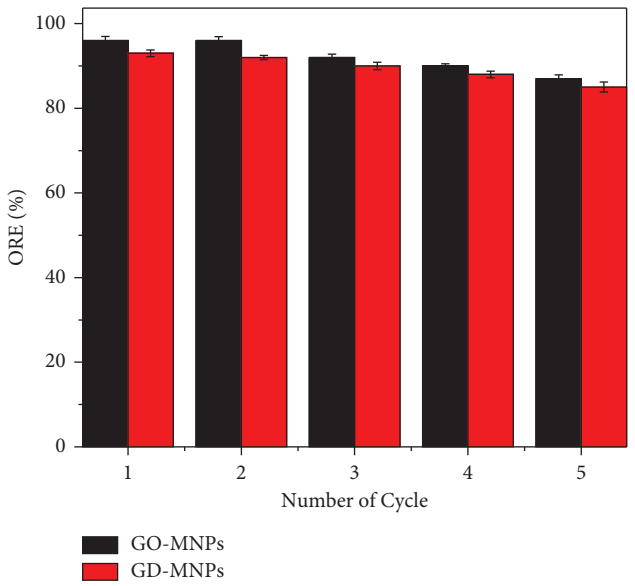

Figure 11: Reusability of GO-MNPs and GD-MNPs using MNP : crude oil ratio of 1 : 4 using method A.

for GO-MNPs and GD-MNPs, respectively, while they declined to 87% and 85% in the fifth cycle. This is possibly due to changes in the hydrophobicity of MNPs with an increasing number of cycles [14].

4. Conclusion

This work aimed to functionalize the surface of MNPs using two unprecedented ILs and apply them for oil spill removal. For that, the epoxy ring of GE was opened with fatty amines, either OA or DA producing the corresponding amines, GEOA and GEDA, respectively. Following this, the produced amines, GEOA and GEDA, were quaternized with AA producing the corresponding ILs, GEOA-IL and GEDA-IL, respectively. GEOA-IL and GEDA-IL were used to functionalize MNP surfaces to generate GO-MNPs and GD-MNPs, respectively. The synthesized MNPs, GO-MNPs and GD-MNPs, were characterized using different techniques, including FTIR, XRD, TGA, TEM, DLS, CA, and VSM. FTIR analysis confirmed the functionality of MNPs with ILs, GEDA-IL and GEOA-IL. The TEM micrographs indicated the nanostructures of GO-MNPs and GD-MNPs with average PS diameters of 11 nm and 8 nm for GO-MNPs and GD-MNPs, respectively. The DLS data exhibited higher PS than that measured with TEM due to the magnetic nature of MNPs in ethanol since they tend to agglomerate. The CA data confirmed the hydrophobicity of GO-MNPs and GD-MNPs. GO-MNPs had higher hydrophobicity than GD-MNPs due to an increase in the hydrophobicity of IL (GEOA) used to functionalize the surface of MNPs when compared to GEDA-IL. The VSM data indicated the response of GO-MNPs and GD-MNPs to the external magnetic fields.

Due to the hydrophobicity of GD-MNPs and GO-MNPs and their response to the external magnet, their ORE values were investigated at different MNP : crude oil ratios using two methods. The data exhibited increased ORE as the MNP ratio increased. In addition, GO-MNPs showed higher ORE than GD-MNPs, which could be linked to increased hydrophobicity due to the use of GEOA-IL containing longer alkyl chains (C18) for the functionality of MNPs than that of GEDA-IL (C12). However, the ORE values produced using the two methods seem similar at high MNP ratios, while the ORE values in method B decrease significantly as MNP ratios decreases, which could be linked to a decrease in the attraction between MNPs and the external magnetic field, especially with the distance between them where the magnet was placed outside the beaker. Furthermore, GO-MNPs and GD-MNPs displayed effective reusability for crude oil removal in five cycles with a limited decrease in their efficiency with increasing cycles, which could be ascribed to the alteration in their hydrophobicity. Finally, the low cost of the synthesized MNPs due to the use of cheap raw materials in short routes, synthesis under mild conditions, their high oil removal efficiency, and their reusability prompt their production in a commercial amount and use them for oil spill combat.

Data Availability

The data used to support the finding of this study are available from the corresponding author upon request.

Conflicts of Interest

The authors declare that they have no conflicts of interest.

Authors' Contributions

Noorah A. Faqihi was responsible for investigation and methodology. Mahmood M. S. Abdullah was responsible for conceptualization, original draft preparation, and reviewing and editing the paper. Mohd Sajid Ali was responsible for reviewing and editing the paper. Hamad A. Al-Lohedan was responsible for investigation, project administration, and resources. Zainab M. Almarhoon was responsible for data curation and resources.

Acknowledgments

The authors acknowledge the financial support through Researchers Supporting Project number (RSPD2023R688), King Saud University, Riyadh, Saudi Arabia.

References

[1] F. Aguilera, J. Méndez, E. Pásaro, and B. Laffon, "Review on the effects of exposure to spilled oils on human health," *Journal of Applied ToxicologyJournal of Applied Toxicology*, vol. 30, no. 4, pp. 291–301, 2010.

[2] B. R. Simonović, D. Arandjelovic, M. Jovanović, B. Kovačević, L. Pezo, and A. Jovanović, "Removal of mineral oil and wastewater pollutants using hard coal," *Chemical Industry And Chemical Engineering Quarterly*, vol. 15, no. 2, pp. 57–62, 2009.

[3] D. Cardona, K. Debs, S. Lemos et al., "A comparison study of cleanup techniques for oil spill treatment using magnetic

nanomaterials," *Journal of Environmental Management*, vol. 242, pp. 362–371, 2019.

[4] A. Fossati, M. Martins Alho, and S. E. Jacobo, "Covalent functionalized magnetic nanoparticles for crude oil recovery," *Materials Chemistry and Physics*, vol. 238, Article ID 121910, 2019.

[5] M. Abdullah, A. U. Rahmah, and Z. Man, "Physicochemical and sorption characteristics of Malaysian Ceiba pentandra (L.) Gaertn. as a natural oil sorbent," *Journal of Hazardous Materials*, vol. 177, no. 1-3, pp. 683–691, 2010.

[6] K. Qiao, W. Tian, J. Bai et al., "Application of magnetic adsorbents based on iron oxide nanoparticles for oil spill remediation: a review," *Journal of the Taiwan Institute of Chemical Engineers*, vol. 97, pp. 227–236, 2019.

[7] B. Singh, S. Kumar, B. Kishore, and T. N. Narayanan, "Magnetic scaffolds in oil spill applications," *Environmental Sciences*, vol. 6, no. 3, pp. 436–463, 2020.

[8] D. Dave and A. E. Ghaly, "Remediation technologies for marine oil spills: a critical review and comparative analysis," *American Journal of Environmental Sciences*, vol. 7, no. 5, pp. 423–440, 2011.

[9] S. Ko, E. S. Kim, S. Park et al., "Amine functionalized magnetic nanoparticles for removal of oil droplets from produced water and accelerated magnetic separation," *Journal of Nanoparticle Research*, vol. 19, pp. 1–14, 2017.

[10] H. Singh, N. Bhardwaj, S. K. Arya, and M. Khatri, "Environmental impacts of oil spills and their remediation by magnetic nanomaterials," *Environmental Nanotechnology, Monitoring & Management*, vol. 14, Article ID 100305, 2020.

[11] A. H. Lu, E. L. Salabas, and F. Schüth, "Magnetic nanoparticles: synthesis, protection, functionalization, and application," *Angewandte Chemie International Edition*, vol. 46, no. 8, pp. 1222–1244, 2007.

[12] W. Wu, Q. He, and C. Jiang, "Magnetic iron oxide nanoparticles: synthesis and surface functionalization strategies," *Nanoscale Research Letters*, vol. 3, no. 11, pp. 397–415, 2008.

[13] M. M. S. Abdullah, A. M. Atta, H. A. Al-Lohedan, H. Z. Alkhathlan, M. Khan, and A. O. Ezzat, "Synthesis of green recyclable magnetic iron oxide nanomaterials coated by hydrophobic plant extracts for efficient collection of oil spills," *Nanomaterials*, vol. 9, no. 10, p. 1505, 2019.

[14] M. M. Abdullah, N. A. Faqihi, H. A. Allohedan, Z. M. Almarhoon, and F. Mohammad, "Fabrication of magnetite nanomaterials employing novel ionic liquids for efficient oil spill cleanup," *Journal of Environmental Management*, vol. 316, Article ID 115194, 2022.

[15] A. M. Atta, A. O. Ezzat, and A. I. Hashem, "Synthesis and application of monodisperse hydrophobic magnetite nanoparticles as an oil spill collector using an ionic liquid," *RSC Advances*, vol. 7, no. 27, pp. 16524–16530, 2017.

[16] M. M. S. Abdullah and H. A. Al-Lohedan, "Alginate-based poly ionic liquids for the efficient demulsification of water in heavy crude oil emulsions," *Fuel*, vol. 320, Article ID 123949, 2022.

[17] M. M. S. Abdullah and H. A. Al-Lohedan, "Demulsification of arabian heavy crude oil emulsions using novel amphiphilic ionic liquids based on glycidyl 4-nonylphenyl ether," *Energy & Fuels*, vol. 33, no. 12, pp. 12916–12923, 2019.

[18] M. M. S. Abdullah and H. A. Al-Lohedan, "Fabrication of environmental-friendly magnetite nanoparticle surface coatings for the efficient collection of oil spill," *Nanomaterials*, vol. 11, p. 3081, 2021.

[19] M. Abdullah, A. M. Atta, H. A. Allohedan, H. Z. Alkhathlan, M. Khan, and A. O. Ezzat, "Green synthesis of hydrophobic magnetite nanoparticles coated with plant extract and their application as petroleum oil spill collectors," *Nanomaterials*, vol. 8, no. 10, p. 855, 2018.

[20] S. Yang, P. Zong, X. Ren, Q. Wang, and X. Wang, "Rapid and highly efficient preconcentration of Eu(III) by core–shell structured Fe3O4@Humic acid magnetic nanoparticles," *ACS Applied Materials & Interfaces*, vol. 4, no. 12, pp. 6891–6900, 2012.

[21] M. Ziegler-Borowska, D. Chełminiak, H. Kaczmarek, and A. Kaczmarek-Kędziera, "Effect of side substituents on thermal stability of the modified chitosan and its nanocomposites with magnetite," *Journal of Thermal Analysis and Calorimetry*, vol. 124, no. 3, pp. 1267–1280, 2016.

[22] C. Schweiger, C. Pietzonka, J. Heverhagen, and T. Kissel, "Novel magnetic iron oxide nanoparticles coated with poly(ethylene imine)-g-poly(ethylene glycol) for potential biomedical application: synthesis, stability, cytotoxicity and MR imaging," *International Journal of Pharmaceutics*, vol. 408, no. 1-2, pp. 130–137, 2011.

[23] A. M. Atta, H. A. Allohedan, and S. A. Al-Hussain, "Functionalization of magnetite nanoparticles as oil spill collector," *International Journal of Molecular Sciences*, vol. 16, no. 12, pp. 6911–6931, 2015.

[24] M. M. S. Abdullah, H. A. Al-Lohedan, and A. M. Atta, "Novel magnetic iron oxide nanoparticles coated with sulfonated asphaltene as crude oil spill collectors," *RSC Advances*, vol. 6, no. 64, pp. 59242–59249, 2016.

[25] A. M. Atta, H. A. Allohedan, and S. A. Al-Hussain, "A versatile one-pot method for the synthesis of amphiphilic bioactive magnetic rosin coated nanoparticles as oil spill collector," *Digest Journal of Nanomaterials and Biostructures*, vol. 10, pp. 745–758, 2015.